MotilA – A Python pipeline for the analysis of microglial fine process motility in 3D time-lapse multiphoton microscopy data

Fabrizio Musacchio [1][¶], **Sophie Crux**[1], **Felix Nebeling**[1], **Nala Gockel**[1], **Falko Fuhrmann**[1], **and Martin Fuhrmann** [1]

1 German Center for Neurodegenerative Diseases (DZNE), Bonn, Germany ¶ Corresponding author

Summary

MotilA is an open-source Python pipeline for quantifying microglial fine-process motility in 4D (TZYX) or 5D (TZCYX) time-lapse fluorescence microscopy data, supporting both single-channel and two-channel acquisition. It was developed for high-resolution *in vivo* multiphoton imaging and supports both single-stack and cohort-scale batch analyses. The workflow performs sub-volume extraction, optional registration and spectral unmixing, a maximum-intensity projection along the Z-axis, segmentation, and pixel-wise change detection to compute the turnover rate (TOR). *MotilA* specifically targets pixel-level process motility rather than object tracking or full morphometry. The code is platform independent, documented with tutorials and example datasets, and released under GPL-3.0.

Statement of need

Microglia are immune cells of the central nervous system and continuously remodel their processes to survey brain tissue and respond to pathology (M. Fuhrmann et al., 2010; Nimmerjahn et al., 2005; Prinz et al., 2019; Tremblay et al., 2010). Quantifying this subcellular motility is important for studies of neuroinflammation, neurodegeneration, and synaptic plasticity. Current practice in many labs relies on manual or semi-manual measurements in general-purpose tools such as Fiji/ImageJ or proprietary software (Carl Zeiss Microscopy GmbH, Accessed 2025; Schindelin et al., 2012). These procedures are time consuming, hard to reproduce, focus on single cells, and are sensitive to user bias (Brown, 2017; Wall et al., 2018). There is no dedicated, open, and batch-capable solution tailored to this task.

MotilA fills this gap with an end-to-end, reproducible pipeline for 3D time-lapse two-channel imaging. It standardizes preprocessing, segmentation, and motility quantification and scales from individual stacks to large experimental cohorts. Unlike Fiji/ImageJ macros or proprietary packages, *MotilA* provides a fully automated non-interactive workflow in Python that applies identical parameters across datasets, logs all intermediate steps, and avoids user-dependent adjustments. This ensures reproducible, bias-minimized, and scalable processing of large 3D time-lapse datasets, including optional motion correction and spectral unmixing. Although optimized for microglia, the approach generalizes to other motile structures that can be reliably segmented across time.

To clarify *MotilA*'s novelty relative to existing analysis approaches, the following table summarizes key differences between *MotilA*, Fiji/ImageJ, and ZEISS ZEN:

Table 1. Comparison of MotilA with commonly used alternatives for microglial motility analysis.

Feature	Fiji/ImageJ	ZEISS ZEN	MotilA
Automation	Limited. User-recorded macros; complex workflows often require manual steps and must be split across several macros.	None. Full user interaction required.	Full. End-to-end non-interactive workflow.
Batch processing	Limited. Macros can process several files in one folder, but they cannot navigate nested directory structures or manage multi-step 3D multi-channel time-series pipelines.	None. Each dataset processed manually.	Full. Metadata-driven cohort processing.
Reproducibility	Moderate. Requires complete manual logging; interactive tuning reduces reproducibility.	Low. Manual adjustments introduce strong user bias.	High. Full parameter logging and deterministic runs.
Scalability	Low. Full-stack RAM loading; no chunked I/O for large 3D data.	Low–medium. Efficient viewing but no automated processing for large time-lapse datasets.	High. Chunked I/O for multi-gigabyte 3D two-channel stacks.
Open-source	Yes (GPL-3.0).	No (proprietary).	Yes (GPL-3.0).

Implementation and core method

Input is a 5D stack in TZCYX or a 4D stack in TZYX order, where T is time, Z is depth, C is channel, and YX are spatial dimensions. *MotilA* does not assume a fixed channel order. Users specify which channel contains microglia and which, if present, provides a structural reference signal, such as a neuronal label. Although the reference channel does not enter the motility computation, it is commonly acquired in microglial imaging because it offers stable features that support robust pre-processing registration of the 3D stack before it is passed to *MotilA*. The additional channel may also be used for optional spectral unmixing in the presence of bleed-through.

For each time point, *MotilA* extracts a user-defined z-sub-volume, optionally performs 3D motion correction and spectral unmixing, and computes a 2D maximum-intensity projection along the Z-axis to enable interpretable segmentation. After thresholding, the binarized projection $B(t_i)$ is compared with $B(t_{i+1})$ to derive a change map
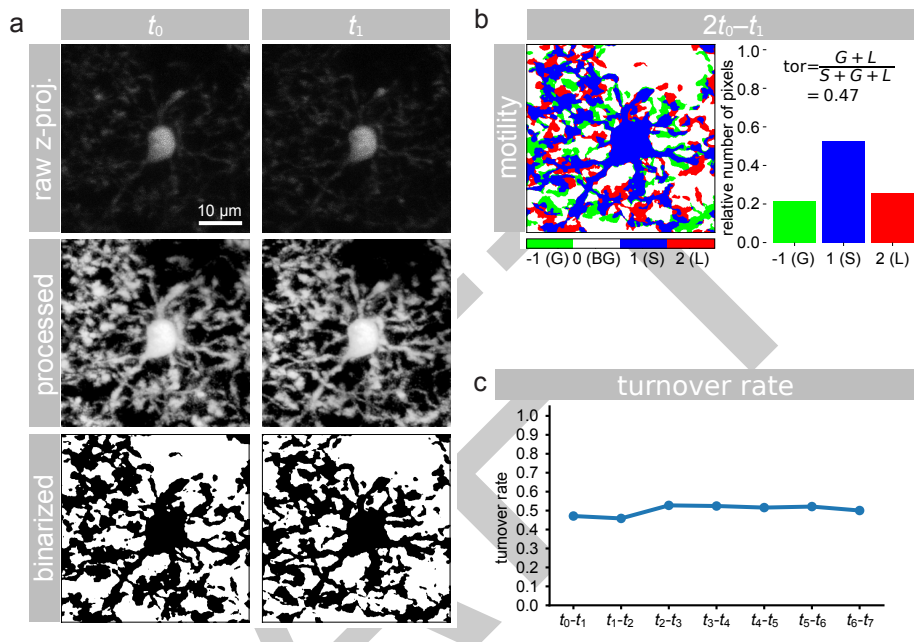
$$\Delta B(t_i) = 2B(t_i) - B(t_{i+1}).$$

Pixels are classified as stable "S" ($\Delta B = 1$), gained "G" ($\Delta B = -1$), or lost "L" ($\Delta B = 2$). From these counts, the turnover rate is defined as

$$TOR = \frac{G + L}{S + G + L},$$

representing the fraction of pixels that changed between consecutive frames. This pixel-based strategy follows earlier microglial motility work (M. Fuhrmann et al., 2010; Nebeling et al., 2023) while providing a fully automated and batchable implementation with parameter logging and diagnostics.

58 The pipeline exposes options for 3D or 2D registration, contrast-limited adaptive histogram
59 equalization, histogram matching across time to mitigate bleaching, and median or Gaussian
60 filtering (Pizer et al., 1987; Virtanen et al., 2020; Walt et al., 2014). Results include segmented
61 images, G/L/S/TOR values, brightness and area traces, and spreadsheets for downstream
62 statistics. Memory-efficient reading and chunked processing of large TIFFs are supported via
63 Zarr (Miles et al., 2025).

Figure 1: Example analysis with MotilA. **a)** z-projected microglial images at two consecutive time points (t_0, t_1), shown as raw, processed, and binarized data. **b)** pixel-wise classification of gained (G), stable (S), and lost (L) pixels used to compute the turnover rate (TOR). **c)** TOR values across time points from the same dataset, illustrating dynamic remodeling of microglial fine processes.

Usage

65 *MotilA* can be called from Python scripts or Jupyter notebooks. Three entry points cover
66 common scenarios: `process_stack` for a single stack, `batch_process_stacks` for a project
67 folder organized by dataset identifiers with a shared metadata sheet, and `batch_collect` to
68 aggregate metrics across datasets. All steps write intermediate outputs and logs to facilitate
69 validation and reproducibility. *MotilA*'s GitHub repository provides tutorials and an example
70 dataset to shorten onboarding.

Applications and scope

72 *MotilA* has been applied to quantify microglial process dynamics in several *in vivo* imaging
73 studies and preprints (Crux et al., 2024; F. Fuhrmann et al., 2024; Gockel et al., 2025). Typical
74 use cases include baseline surveillance behavior, responses to neuroinflammation or genetic
75 perturbations, and deep three-photon imaging where manual analysis is impractical. The
76 binarize-and-compare principle can in principle be adapted to other structures such as dendrites
77 or axons when segmentation across time is robust.

Limitations

79 Using 2D projections simplifies processing but sacrifices axial specificity and can merge
80 overlapping structures. Segmentation quality determines accuracy and can be affected by

81 vessels, low signal-to-noise ratios, or strong intensity drift. The current spectral unmixing is a
82 simple subtraction; advanced approaches may be needed for some fluorophores. *MotilA* targets
83 pixel-level process motility rather than object-level tracking or full morphometry.

84 Using 2D Z-projections confines motility quantification to the XY plane, but this reflects
85 practical constraints of two-photon microglial imaging. Axial resolution degrades with imaging
86 depth, yielding elongated point-spread functions and reduced contrast along Z, which makes
87 voxel-wise 3D segmentation of thin microglial processes unreliable. Maximum-intensity pro-
88 jection increases effective signal per pixel and follows established practice in earlier microglial
89 motility work (see, e.g., M. Fuhrmann et al. (2010); Nebeling et al. (2023)). This approach
90 necessarily sacrifices axial specificity and can merge structures that overlap in Z, particularly
91 in densely populated regions, which are best avoided by selecting a sub-volume with minimal
92 axial overlap. Fully 3D motility analysis would require volumetric segmentation, morphological
93 reconstruction, and substantially higher memory and computational resources and is therefore
94 out of scope for the current version of *MotilA*.

95 Beyond the inherent limitations of Z-projection, segmentation quality critically affects accuracy
96 and can be influenced by blood vessels, low signal-to-noise ratios, and strong intensity drift
97 across time. The current spectral unmixing is implemented as a simple subtraction and may be
98 insufficient for fluorophores with complex spectral overlap. *MotilA* targets pixel-level process
99 motility rather than object-level tracking or full morphometry, and its interpretability depends
100 on reliable and consistent segmentation across frames.

Example dataset

102 The repository includes two *in vivo* two-photon stacks from mouse frontal cortex formatted for
103 use with *MotilA* (Gockel et al., 2025). Each stack contains eight time points at five-minute
104 intervals, two channels for microglia and neurons, and approximately sixty z-planes at one
105 micrometer steps in a field of view of about 125 by 125 micrometers. The example reproduces
106 the full analysis, including projections, segmentation, change maps, brightness traces, and
107 TOR over time, and serves as a template for cohort-level workflows.

Availability

109 Source code, documentation, tutorials, and issue tracking are hosted at: https://github.com/
110 FabrizioMusacchio/motila. The software runs on Windows, macOS, and Linux with Python 3.9
111 or newer and standard scientific Python stacks. It is released under GPL-3.0, and contributions
112 via pull requests or issues are welcome.

Acknowledgements

References

123 Brown, D. L. (2017). Bias in image analysis and its solution: Unbiased stereology. *Journal of*
124 *Toxicologic Pathology*, *30*(3), 183–191. https://doi.org/10.1293/tox.2017-0013

125 Carl Zeiss Microscopy GmbH. (Accessed 2025). *ZEISS ZEN Microscopy Software*. https:
126 //www.zeiss.com/metrology/en/software/zeiss-zen-core.html

127 Crux, S., Roggan, M. D., Poll, S., Nebeling, F. C., Schiweck, J., Mittag, M., Musacchio, F.,
128   Steffen, J., Wolff, K. M., Baral, A., Witke, W., Gurniak, C., Bradke, F., & Fuhrmann,
129   M. (2024). Deficiency of actin depolymerizing factors ADF/Cfl1 in microglia decreases
130   motility and impairs memory. *bioRxiv*. https://doi.org/10.1101/2024.09.27.615114

131 Fuhrmann, F., Nebeling, F. C., Musacchio, F., Mittag, M., Poll, S., Müller, M., Giovannetti, E.
132   A., Maibach, M., Schaffran, B., Burnside, E., Chan, I. C. W., Lagurin, A. S., Reichenbach,
133   N., Kaushalya, S., Fried, H., Linden, S., Petzold, G. C., Tavosanis, G., Bradke, F., &
134   Fuhrmann, M. (2024). Three-photon in vivo imaging of neurons and glia in the medial
135   prefrontal cortex with sub-cellular resolution. *bioRxiv*. https://doi.org/10.1101/2024.08.
136   28.610026

137 Fuhrmann, M., Bittner, T., Jung, C. K. E., Burgold, S., Page, R. M., Mitteregger, G., Haass,
138   C., LaFerla, F. M., Kretzschmar, H., & Herms, J. (2010). Microglial Cx3cr1 knockout
139   prevents neuron loss in a mouse model of alzheimer's disease. *Nature Neuroscience*, *13*(4),
140   411–413. https://doi.org/10.1038/nn.2511

141 Gockel, N., Nieves-Rivera, N., Druart, M., Jaako, K., Fuhrmann, F., Rožkalne, R., Musacchio,
142   F., Poll, S., Jansone, B., Fuhrmann, M., & Magueresse, C. L. (2025). *Example datasets for*
143   *microglial motility analysis using the MotilA pipeline*. Zenodo. https://doi.org/10.5281/
144   zenodo.15061566

145 Miles, A., jakirkham, Hamman, J., Orfanos, D. P., Stansby, D., Bussonnier, M., Moore,
146   J., Bennett, D., Augspurger, T., Rzepka, N., Cherian, D., Verma, S., Bourbeau, J.,
147   Fulton, A., Abernathey, R., Lee, G., Spitz, H., Kristensen, M. R. B., Jones, M., &
148   Schut, V. (2025). *Zarr-developers/zarr-python: v3.0.6* (Version v3.0.6). Zenodo. https:
149   //doi.org/10.5281/zenodo.3773449

150 Nebeling, F. C., Poll, S., Justus, L. C., Steffen, J., Keppler, K., Mittag, M., & Fuhrmann,
151   M. (2023). Microglial motility is modulated by neuronal activity and correlates with
152   dendritic spine plasticity in the hippocampus of awake mice. *eLife*, *12*, e83176. https:
153   //doi.org/10.7554/eLife.83176

154 Nimmerjahn, A., Kirchhoff, F., & Helmchen, F. (2005). Resting microglial cells are highly
155   dynamic surveillants of brain parenchyma in vivo. *Science*, *308*(5726), 1314–1318. https:
156   //doi.org/10.1126/science.1110647

157 Pizer, S. M., Amburn, E. P., Austin, J. D., Cromartie, R., Geselowitz, A., Greer, T., Haar
158   Romeny, B. ter, Zimmerman, J. B., & Zuiderveld, K. (1987). Adaptive histogram equaliza-
159   tion and its variations. *Computer Vision, Graphics, and Image Processing*, *39*(3), 355–368.
160   https://doi.org/10.1016/S0734-189X(87)80186-X

161 Prinz, M., Jung, S., & Priller, J. (2019). Microglia biology: One century of evolving concepts.
162   *Cell*, *179*(2), 292–311. https://doi.org/10.1016/j.cell.2019.08.053

163 Schindelin, J., Arganda-Carreras, I., Frise, E., Kaynig, V., Longair, M., Pietzsch, T., Preibisch,
164   S., Rueden, C., Saalfeld, S., Schmid, B., & others. (2012). Fiji: An open-source platform
165   for biological-image analysis. *Nature Methods*, *9*(7), 676–682. https://doi.org/10.1038/
166   nmeth.2019

167 Tremblay, M.-È., Lowery, R. L., & Majewska, A. K. (2010). Microglial interactions with
168   synapses are modulated by visual experience. *PLOS Biology*, *8*(11), 1–16. https://doi.org/
169   10.1371/journal.pbio.1000527

170 Virtanen, P., Gommers, R., Oliphant, T. E., Haberland, M., Reddy, T., Cournapeau, D.,
171   Burovski, E., Peterson, P., Weckesser, W., Bright, J., Walt, S. J. van der, Brett, M.,
172   Wilson, J., Millman, K. J., Mayorov, N., Nelson, A. R. J., Jones, E., Kern, R., Larson, E., …
173   Contributors, S. 1.0. (2020). SciPy 1.0: Fundamental algorithms for scientific computing
174   in python. *Nature Methods*, *17*, 261–272. https://doi.org/10.1038/s41592-019-0686-2

175 Wall, E., Blaha, L. M., Paul, C. L., Cook, K., & Endert, A. (2018). Four perspectives on

human bias in visual analytics. In G. Ellis (Ed.), *Cognitive biases in visualizations* (pp. 29–42). Springer International Publishing. https://doi.org/10.1007/978-3-319-95831-6_3

Walt, S. van der, Schönberger, J. L., Nunez-Iglesias, J., Boulogne, F., Warner, J. D., Yager, N., Gouillart, E., Yu, T., & contributors, the scikit-image. (2014). Scikit-image: Image processing in python. *PeerJ*, *2*, e453. https://doi.org/10.7717/peerj.453